A BIOPHYSICAL MODEL OF SPIKE-TIMING DEPENDENT PLASTICITY

Florentin Wörgötter, Bernd Porr and Ausra Saudargiene
Department of Psychology, University of Stirling,
Stirling FK9 4LA, Scotland,
<worgott,bp1,ausra>@cn.stir.ac.uk

ABSTRACT

Rather early first indications arose that temporal order of pre- and postsynaptic spikes is important in Hebbian learning (Levy and Steward, 1983). Later this was termed spike-timing dependent plasticity (STDP), which refers to the observation that many synapses will decrease in strength when the postsynaptic signal precedes the presynaptic signal (defined here as: $T < 0$), while they will grow if the temporal order is reversed (thus, $T > 0$) (Markram et al., 1997; Magee and Johnston, 1997). T denotes the temporal interval between post- and presynaptic signals ($T := t_{post} - t_{pre}$). Recently we had introduced a very simple and linear algorithm for temporal sequence learning in robots, called "ISO-learning" (Porr and Wörgötter, 2003), which reproduced the characteristic, anti-symmetrical weight change curve found in STDP, albeit on a much longer time scale (compare Fig. 1 C). Here we are setting out to implement ISO-learning in the context of a simple, single-compartment neuron model showing that it is basically compatible with the biophysics of synaptic plasticity. The central finding of this model is that the ISO-learning rule leads in a robust and generic way to STDP, while the shape of the input signals distinctively influences the shape of the weight change curve.

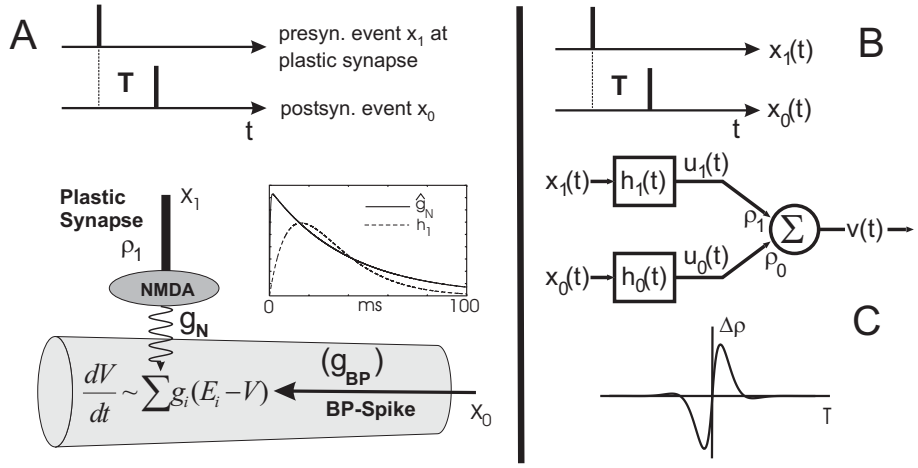

Figure 1: Schematic diagram of the model. A) Components of the membrane model. The inset shows how to match the NMDA-conductance function $\hat{g}_N$ (Eq. 1) with a resonator impulse response h_1. B) Components of ISO-learning. C) Typical weight change curve obtained with ISO-learning.

Components of the membrane model: The model represents a small, non-spiking, dendritic compartment with a single synapse ρ_1 which was assumed as the so called "plastic synapse (PS)" on which the influence of the ISO-learning rule was tested. This synaptic connection takes the shape of an NMDA characteristic and the conductance g_N of NMDA channels was modeled by:

$$g_N(t) = \bar{g}_N \;\; \hat{g}_N(t) = \bar{g}_N \;\; \frac{e^{-t/\tau_1} - e^{-t/\tau_2}}{1 + \eta[Mg^{2+}]\, e^{-\gamma V}} \tag{1}$$

This slightly more complex notation is used, because we will need the normalized conductance time functions $\hat{g}_N(t)$ on their own below when introducing the learning rule. Parameter were taken from the standart literture Koch (1999). The conventional membrane equation was used to determine the momentarily existing membrane potential.
The influence of the NMDA-component on the membrane potential is dependent on the membrane's depolarization level. We assume in this model that this is determined by the post-synaptic

activity which arises from a back-propagating spike (BP-spike). Other synaptically arising influences have also been tested but cannot be described in this short paper.
Components of ISO-learning: Fig. 1 B shows the circuit diagram of rate-based ISO-learning for only two (δ-pulse) inputs $x_0,\ x_1$ (for a more general description see Porr and Wörgötter 2003). The inputs are first band-pass filtered by means of heavily damped resonators h. The transformed inputs $u_{0,1} = x_{0,1} * h$ converge onto the learning unit with weights $\rho_{0,1}$ and its output is given by $v = \rho_0 u_0 + \rho_1 u_1$. The ISO-learning rule is given by: $\frac{d}{dt}\rho_1 = \mu u_1 v'$ with $\mu \ll 1$.
Associating the membrane model to ISO-learning: The band-pass filter operation h_1 is represented by the conductance function g of the plastic synapse and we define $h_1(t) := \hat{g}_N$. Since we are only dealing with spike trains modeled as δ-functions we get $u_1(t) = h_1(t) = \hat{g}_N$. Corresponding curves are shown in the inset of Fig. 1 A. The output v is the membrane potential V. As a consequence of these settings the learning rule of ISO-learning is rephrased in the context of this model to:

$$\frac{d}{dt}\rho_1 = \mu u_1 v' = \mu\ \hat{g}_N\ V' \tag{2}$$

For the actual weight change $\Delta\rho$ obtained with one spike pair at the inputs we integrate as usual: $\Delta\rho_1 = \int_0^t \frac{d\rho_1}{dt} dt$. The learning rate μ takes the unit of Volt^{-1}, because this way $\Delta\rho$ is rendered unit-free.

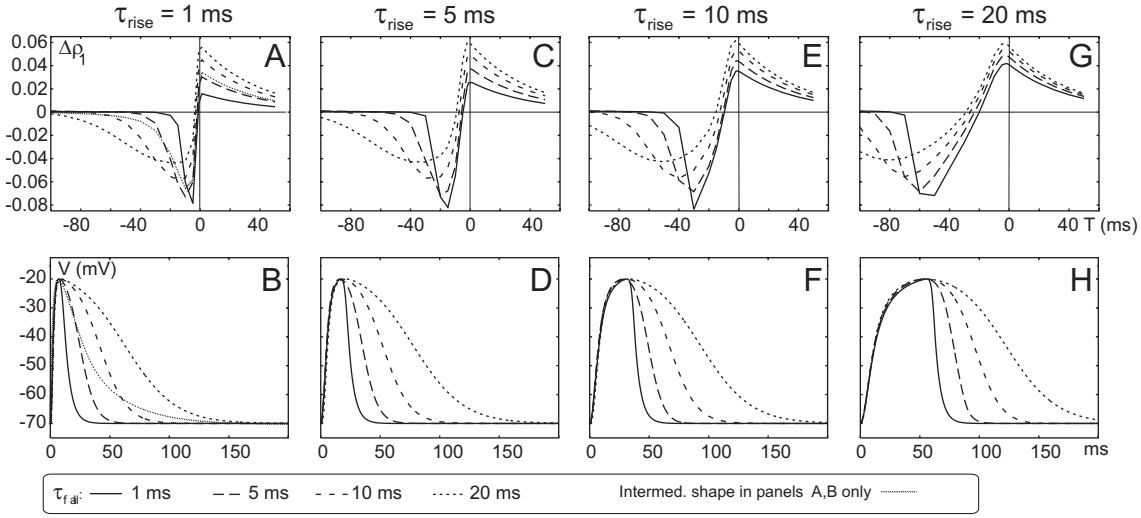

Figure 2: Weight change curves obtained with different BP-spikes as depolarization source. Top panels show the weight change curves and bottom panels the BP-spikes with which they were obtained, parameterized with different rise and fall-times. Panels A,B also contain one example obtained with a BP-spike with intermediate shape This spike starts with the shape of the first BP-spike in panel B and ends with the shape of the last spike.

Results: Fig. 2 shows 17 weight change curves and the BP-spikes with which they were obtained. Note, (some of) these spike shapes do not necessarily reflect realistic BP-spike shapes. Instead, this modeling exercise is meant to cover a rather complete range of composable shapes such that the characteristics of a weight change curve resulting from any other BP-spike shape can be inferred from this diagram.
In general, we observe that the negative part of the weight change curve dominates in most cases across all panels, which is in accordance with physiology (Debanne et al., 1998).
By comparing the curves *within* each panel, it can be seen that increasing fall-times of the BP-spike mainly lead to an increase of the positive peak of the weight change curve while the negative peak becomes smaller but more spread out towards negative values of T.
By comparing curves *across* panels one can assess the influence of increasing rise-times. Here we observe that the typical STDP-shape of the curves in panel A (zero crossing at about $T = 0\ ms$) turns into pure Hebbian learning for values of $T > -20\ ms$ for a rather shallow rise-time. Such shallow rise-times may indeed occur at distal dendrites where - discounting possible active processes - the membrane capacitance has smeared out a BP-spike substantially (Magee and Johnston, 1997). This result is of some theoretical interest, because it shows that we do not have to alter the learning rule in order to get either differential- (STDP-like curve) or plain-Hebbian (unimodal curve) learning. A changing input characteristic will do the trick already.

The one example of a BP-spike with intermediate shape (panels A,B) shows - quite expectedly so - that gradual spike-shape transitions will also lead to gradual transitions of the shape of the weight change curves. This supports the notion that other shapes of weight change curves can be basically inferred from these examples.
Let us also consider the influence of different resting potentials which will affect the NMDA channel. Fig. 3 A shows that this influence is rather weak. This is due to the fact that the transient depolarization coming from the BP-spike now dominates the artificially introduced tonic depolarization of the resting membrane level.

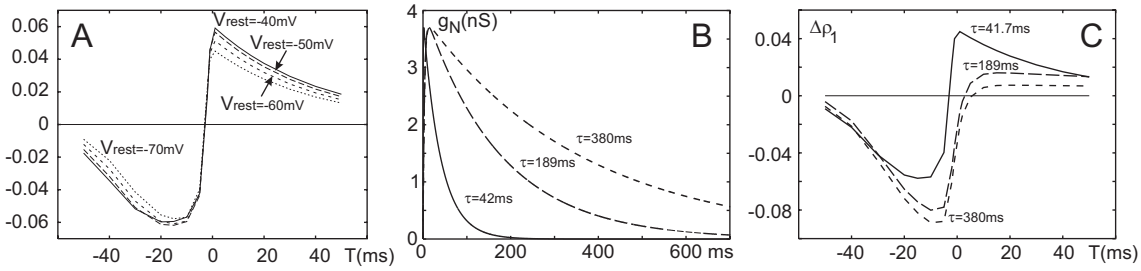

Figure 3: Learning curves obtained with different resting membrane potentials (A) or different NMDA characteristics (B,C). A) Influence of the resting potential indicated by the labels on the curves. B) conductance of the NMDA synapse at $+40\ mV$ voltage clamp. C) Weight change curves.

It is known that during development the relative frequency of different NMDA receptor types (NMDAR$_A$ versus NMDAR$_B$) changes. This influences the electrophysiological properties of the NMDA-channel. Fig. 3 A,B shows three different NMDA-characteristics, the steepest reflecting an adult stage. The other two stages are observed during development at postnatal days 26-29 ($\tau_{decay} = 189\ ms$) and 37-38 ($\tau_{decay} = 380\ ms$) in ferret. The single decay values for τ_{decay} were taken from Roberts and Ramoa (1999), but we still modeled the NMDA characteristic using Eq. 1 by fitting our two τ-values to yield the curves reported in the report of Roberts & Ramoa. To obtain the weight change curves we used a BP-spike with short rise-time and medium fall-time. Interestingly we observe that both "young" NMDA-synapses yield rather asymmetrical weight change curves with a strongly dominated LTD part. To our knowledge so far very little is known about the actual physiological learning characteristics of early synapses. There are, however, indications that synaptic elimination dominates the early developmental stages. The theoretical results obtained with our learning rule would possibly point towards this direction.
Discussion - Relations to Biophysics: The learning rule consists of two components. In most cases, the membrane potential is strongly dominated by the shape of the BP-spike at the moment of pairing, while the contribution of the plastic synapse (or other synapses) can be neglected. This makes V' a post-synaptic quantity. Given that $V' = \frac{I}{C}$, we note that the learning rule can be rewritten also as $\frac{d\rho}{dt} = \frac{\mu}{C}\hat{g}\frac{dQ}{dt}$. This shows that charge transfer $\frac{dQ}{dt}$ across the (post-synaptic) membrane is a major driving force of learning and it seems reasonable to assume that part of $\frac{dQ}{dt}$ represents the calcium flow. As the first term of the learning rule, we have used the normalized NMDA conductance function $\hat{g}_N$, which, thus, represents the band-pass filtered input u_1 of ISO-learning's response to a δ-pulse input. We would argue that $\hat{g}_N$ essentially subsumes the *time-course* of all processes which occur for an NMDA receptor outside or directly at the membrane; thus all pre-synaptic events. Thus, our learning rule uses a product of a pre-synaptic ($\hat{g}$) and a post-synaptic (V') influence.
In summary, our model falls in-between the rather abstract models of, for example, (Gerstner et al., 1996; Song et al., 2000; Rubin et al., 2001) and the more kinetically oriented models of (Senn et al., 2000; Castellani et al., 2001; Karmarkar and Buonomano, 2002; Shouval et al., 2002). We believe that this study may help to further our understanding of more complex (compartmentalized and/or kinetic) models because the question of how a certain STDP curve arises is reduced to the question of how the cellular parameters lead to the underlying input signal shapes.

Acknowledgements: The authors acknowledge the support from SHEFC INCITE. We are grateful to B. Graham, L. Smith and D. Sterratt for their helpful comments on this manuscript.

References

Castellani, G. C., Quinlan, E. M., Cooper, L. N., and Shouval, H. Z. (2001). A biophysical model of bidirectional synaptic plasticity: Dependence on AMPA and NMDA receptors. *Proc. Natl. Acad. Sci. (USA)*, 98(22):12772–12777.

Debanne, D., Gahwiler, B., and Thompson, S. (1998). Long-term synaptic plasticity between pairs of individual CA3 pyramidal cells in rat hippocampal slice cultures. *J. Physiol. (Lond.)*, 507:237–247.

Gerstner, W., Kempter, R., van Hemmen, J. L., and Wagner, H. (1996). A neuronal learning rule for sub-millisecond temporal coding. *Nature*, 383:76–78.

Karmarkar, U. R. and Buonomano, D. V. (2002). A model of spike-timing dependent plasticity: One or two coincidence detectors? *J. Neurophysiol.*, 88:507–513.

Koch, C. (1999). *Biophysics of Computation*. Oxford University Press.

Levy, W. B. and Steward, O. (1983). Temporal contiguity requirements for long-term associative potentiation/depression in the hippocampus. *Neurosci.*, 8:791–797.

Magee, J. C. and Johnston, D. (1997). A synaptically controlled, associative signal for Hebbian plasticity in hippocampal neurons. *Science*, 275:209–213.

Markram, H., Lübke, J., Frotscher, M., and Sakmann, B. (1997). Regulation of synaptic efficacy by coincidence of postsynaptic APs and EPSPs. *Science*, 275:213–215.

Porr, B. and Wörgötter, F. (2003). Isotropic sequence order learning. *Neural Comp.*, 15:831–864.

Roberts, E. B. and Ramoa, A. S. (1999). Enhanced NR2A subunit expression and decreased NMDA receptor decay time at the onset of ocular dominance plasticity in the ferret. *J. Neurophysiol.*, 81:2587–2591.

Rubin, J., Lee, D. D., and Sompolinsky, H. (2001). Equilibrium properties of temporally asymmetric Hebbian plasticity. *Phys. Rev. Lett.*, 86(2):364–367.

Senn, W., Markram, H., and Tsodyks, M. (2000). An algorithm for modifying neurotransmitter release probability based on pre-and postsynaptic spike timing. *Neural Comp.*, 13:35–67.

Shouval, H. Z., Bear, M. F., and Cooper, L. N. (2002). A unified model of NMDA receptor-dependent bidirectional synaptic plasticity. *Proc. Natl. Acad. Sci. (USA)*, 99(16):10831–10836.

Song, S., Miller, K. D., and Abbott, L. F. (2000). Competitive Hebbian Learning through spike-timing-dependent synaptic plasticity. *Nature Neurosci.*, 3:919–926.